

Dapped ends of prestressed concrete thin-stemmed members: Part 1, experimental testing and behavior

Amir W. Botros, Gary J. Klein, Gregory W. Lucier, Sami H. Rizkalla, and Paul Zia

- This paper describes the behavior of dapped ends of prestressed concrete thin-stemmed members based on an extensive experimental program conducted to identify the most effective reinforcement schemes and develop design guidelines for dapped ends.
- Experimental research findings presented in this paper were used to develop design guidelines that are presented in “Dapped Ends of Prestressed Concrete Thin-Stemmed Members: Part 2, Design,” which also appears in the March–April 2017 *PCI Journal*.
- The experimental results indicated that the extent of cracking at service load, the ultimate strength, and the failure mode are influenced by the reinforcement arrangement at the dapped end.

Precast concrete double-tee beams with thin stems are widely used for parking structures and other buildings. Frequently, the end supports are dapped such that the bottom of the stem of the double tees is level with the bottom of the supporting ledger beam. The dapped connection detail is important at crossovers between spans in parking structures where the overall depth of the double tee needs to be flush with the supporting ledger beam.

A dapped beam relies on a reduced section to support the member. The notch itself is known as the dap, and the reduced concrete section remaining above the dap is referred to as the nib. **Figure 1** shows a dapped-end connection typically used for parking structures.

The design and construction of dapped double tees is challenging for several reasons. The strength of a dapped end depends on the development of a load path that transfers the vertical shear and moment in the full section of the member to the bearing reactions beneath the shallower nib. The pretensioning strands, stem reinforcement, and intersecting deformed reinforcement are all competing for space in stems that are only about 5 in. (125 mm) wide. Design of the nib requires consideration of high shear stresses, which are greater than elsewhere in the member. Unlike bottom-supported members, compression from the bearing reaction is not available to help resist longitudinal splitting where the pretensioning strand and deformed reinforcement overlap. While dapped-end reinforcement details generally provide adequate strength, undesirable

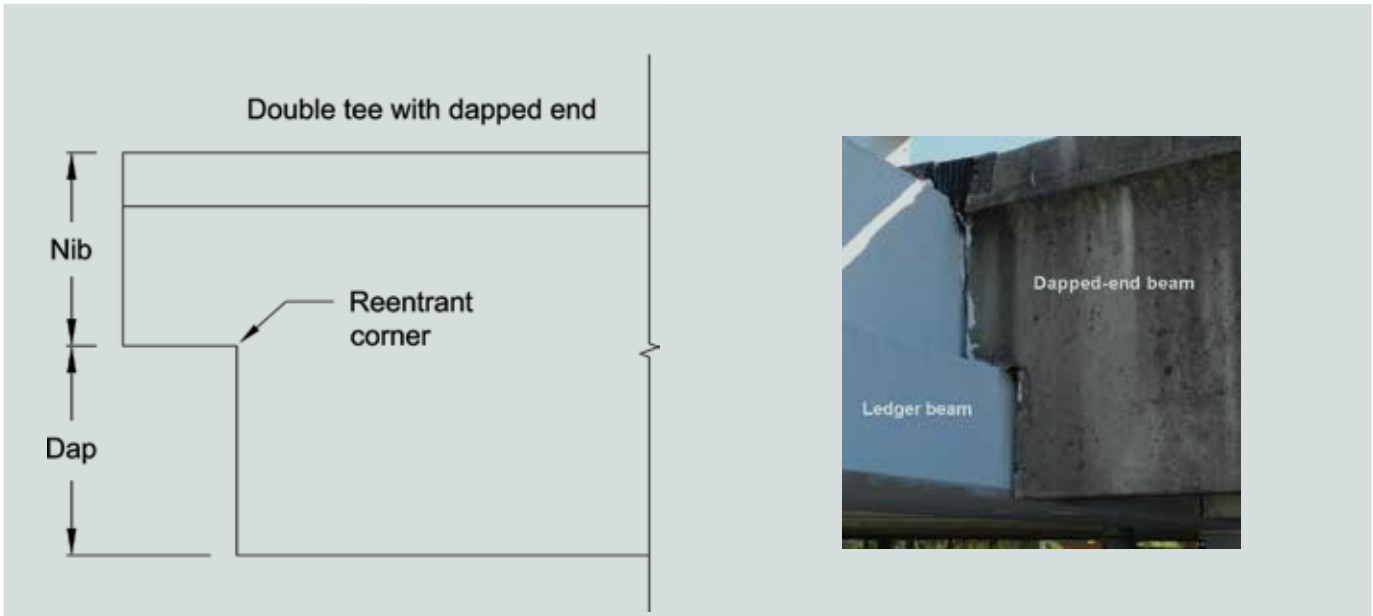


Figure 1. Typical dapped-end beam and dapped-end connection used for parking structures.

cracks are often observed at service loading. In some cases, the cracks may also be attributed to poor design or construction practices.

The current design procedure for dapped-end connections, outlined in the seventh edition of the *PCI Design Handbook: Precast and Prestressed Concrete*,¹ is based on the research of Mattock and Chan.² The design method is based on the equilibrium of forces acting across potential failure planes and conservatively treats the dapped-end details as reinforced concrete inverted corbel details.

The *PCI Design Handbook* illustrates typical dapped-end reinforcement details and potential failure planes that have been observed in dapped double-tee beams (**Fig. 2**). The bars labeled A_{sh} are referred to as *hanger reinforcement*, with anchorage provided by the horizontal extension A'_{sh} bent toward the full-depth section of the beam. The hanger reinforcement serves to transfer the vertical reaction at the nib to the full section of the beam and to resist the diagonal tension cracking from the reentrant corner (crack 3) and in the full-depth section (crack 5) (top of Fig. 2). The bars labeled A_s are referred to as *nib flexural reinforcement* and are required for resisting the cantilever bending and axial tension in the nib. The *PCI Design Handbook* requires that the A_s and A'_{sh} reinforcement be extended past the critical diagonal crack failure plane indicated as crack 5, a distance that cannot be less than the development length of the bars ℓ_d . The bars labeled A_h and A_v are required for resisting the diagonal tension cracking in the nib indicated as crack 4.

The thin stems of prestressed tee members are usually too tight to accommodate hanger reinforcement in the shape of closed stirrups (top of Fig. 2). Therefore, a bar bent in a

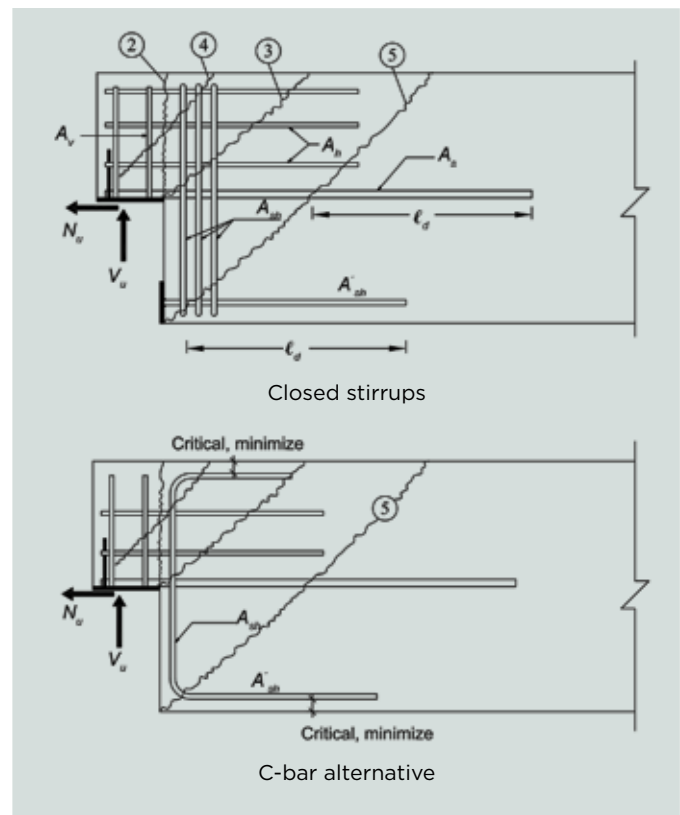


Figure 2. Potential failure modes and required reinforcement in dapped-end connections.

Source: PCI Industry Handbook Committee (2010)

Note: A_h = area of shear-friction reinforcement across vertical crack at dapped ends and corbels; A_s = area of nib flexural reinforcement; A_{sh} = area of hanger reinforcement for dapped end; A'_{sh} = area of horizontal extension of hanger reinforcement; A_v = area of diagonal tension reinforcement; ℓ_d = development length of reinforcement; N_u = factored horizontal or axial force; V_u = factored vertical reaction at end of beam.

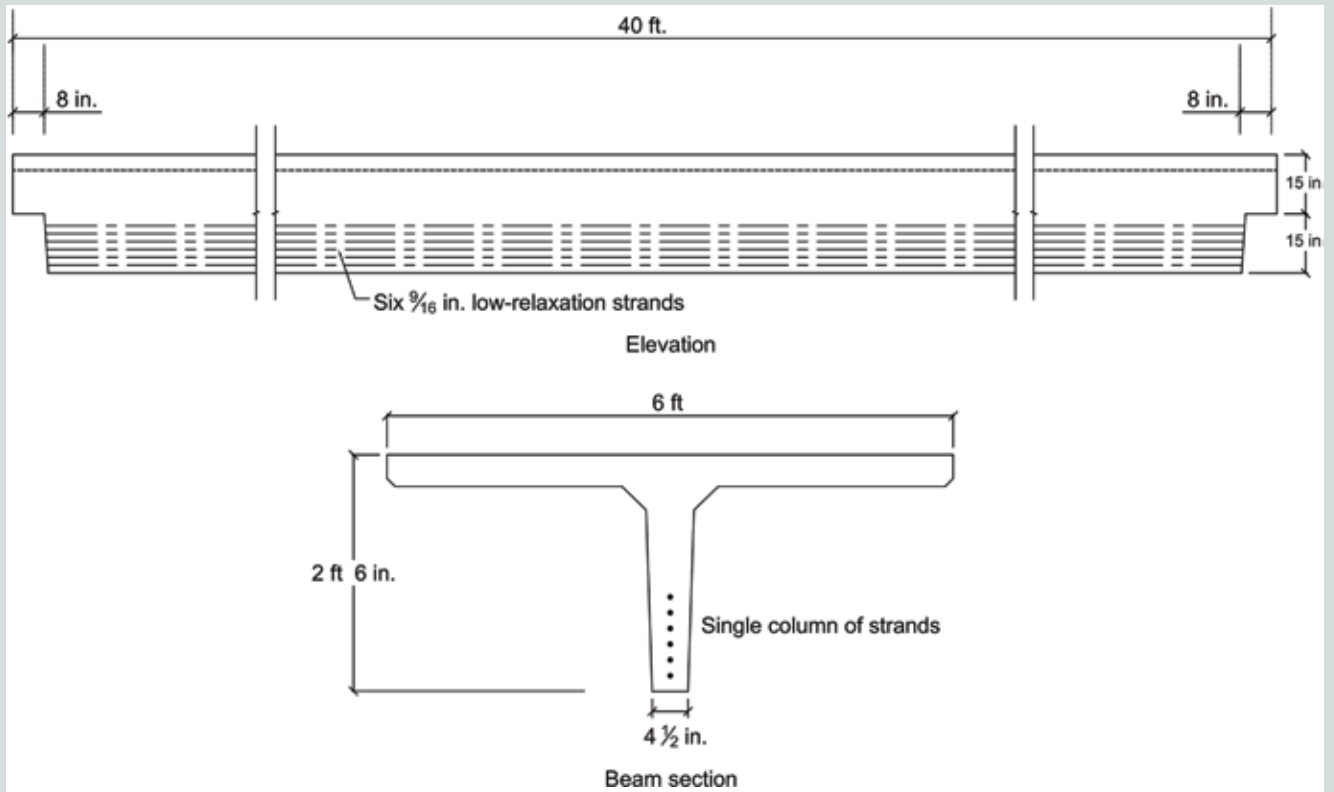


Figure 3. Elevation and cross section of test specimens. Note: 1 in. = 25.4 mm; 1 ft = 0.305 m.

C shape, commonly known as C bar, is used as a common alternative (bottom of Fig. 2). The bar is anchored at the upper end by extending its upper leg in the compression zone while the lower end is anchored by extending it along the bottom of the web.

While many successful reinforcement details have been developed for dapped-end connections, the industry has experienced problems with structural distress and failures at these connections. The observed problems generally fall into four categories: service cracking at the reentrant corner, distress related to use of C-bar hanger reinforcement, bearing region distress, and splitting cracks near the bottom of the full section.

Mattock and Theyro³ conducted an experimental program to investigate the behavior of five dapped-end reinforcement schemes for thin-stemmed prestressed concrete members. The study tested five different reinforcement details using 16 ft (4.9 m) long beams subjected to a combination of shear and outward tension typically induced at the bearing plate. The research concluded that the inclined hanger reinforcement detail is the most effective detail in terms of strength and crack control. Mattock and Theyro³ also indicated that passing prestressing strands through the nib section reduces the crack width at service loads.

Nanni and Huang⁴ introduced an alternative reinforcement detail for the dapped ends of prestressed concrete double tees that was found to be effective in terms of strength and reduction of crack width at service load.

In 2012, Logan sponsored a test program⁵ of dapped tees to examine the performance of eight different reinforcement schemes for the dapped ends using four 30 ft (9 m) long prestressed dapped-end single-tee beams. The results of these tests were presented by Forsyth in his thesis,⁵ which indicated that the failure of all specimens occurred through the full depth of the section across a critical diagonal crack. The results also indicated that passing one strand through the nib improved cracking performance compared with an identical specimen without strands in the nib.

There exists a substantial body of literature regarding the analysis, design, and testing of dapped-end thin-stemmed members.^{6,7,8} As part of the research by Klein, Andrews, and Holloway,⁷ an industry survey of producers in 2012 revealed that at least six different reinforcement schemes are being used in the dapped ends of double-tee beams. The results of the survey also indicated that the C-shaped hanger reinforcement is the most common reinforcing scheme used in the dapped ends of the double tees.

Table 1. Test matrix for the experimental program

| Specimen | Parameter | Design loads | Dap reinforcing scheme | Strand pattern | Hanger steel | Strands in nib | Concrete strength, psi | Web shear reinforcement | | Nib height, in. | Corner angle | Splice length, in. |
|----------|-------------------------|--------------|------------------------|----------------|--------------|----------------|------------------------|-------------------------|--------------|-----------------|--------------|--------------------|
| | | | | | | | | Size | Spacing, in. | | | |
| 1A | Control | Moderate | Vertical L | Single column | Two no. 5 | 0 | 6000 | W4 | 6 | 15 | No | 36 |
| 1B | | High | Vertical L | Single column | Four no. 4 | 0 | 6000 | W6 | 4 | 15 | No | 36 |
| 2A | Reinforcement scheme | Moderate | Vertical Z | Staggered | One no. 7 | 0 | 6000 | W4 | 6 | 15 | Yes | 36 |
| 2B | | High | Vertical Z | Staggered | One no. 8 | 0 | 6000 | W6 | 4 | 15 | No | 36 |
| 3A | | Moderate | Inclined L | Single column | Two no. 5 | 0 | 6000 | W4 | 6 | 15 | No | 36 |
| 3B | | High | Inclined L | Single column | Four no. 4 | 0 | 6000 | W6 | 4 | 15 | No | 36 |
| 4A | | Moderate | Custom WWR | Staggered | Two D31 | 0 | 6000 | W4 | 6 | 15 | No | 45 |
| 4B | | Moderate | Vertical C | Staggered | One no. 7 | 0 | 6000 | W4 | 6 | 15 | No | 36 |
| 5A | Nib prestress | Moderate | Vertical Z | Staggered | One no. 7 | 2 | 6000 | W4 | 6 | 15 | Yes | 36 |
| 5B | | High | Vertical Z | Staggered | One no. 8 | 2 | 6000 | W6 | 4 | 15 | No | 36 |
| 6A | Concrete strength | High | Vertical Z | Single column | Two no. 6 | 0 | 10,000 | W6 | 4 | 15 | No | 36 |
| 6B | | High | Vertical L | Single column | Four no. 4 | 0 | 10,000 | W6 | 4 | 15 | No | 36 |
| 7A | Web shear reinforcement | High | Custom WWR | Single column | Two D26 | 0 | 6000 | W8 | 4 | 15 | No | 45 |
| 7B | | High | Vertical C | Single column | Two no. 5 | 0 | 6000 | W8 | 4 | 15 | No | 36 |
| 8A | Nib height | Moderate | Vertical L | Single column | Two no. 5 | 0 | 6000 | W4 | 6 | 12 | No | 36 |
| 8B | | Moderate | None | Single column | None | 4 | 6000 | W4 | 6 | 24 | No | 36 |
| 9A | Splice length | Moderate | Vertical L | Single column | Two no. 5 | 0 | 6000 | W4 | 6 | 15 | No | 60 |
| 9B | | Moderate | Vertical L | Single column | Two no. 5 | 0 | 6000 | W4 | 6 | 15 | No | 15 |
| 10A | Reinforcement scheme | Moderate | CZ | Staggered | Two no. 5 | 0 | 6000 | W4 | 6 | 15 | No | 36 |
| 10B | Pocket nib detail | Moderate | Vertical Z | Staggered | One no. 7 | 0 | 6000 | W4 | 6 | 15 | No | 36 |

Note: WWR = welded-wire reinforcement. No. 4 = 13M; no. 5 = 16M; no. 6 = 19M; no. 7 = 22M; no. 8 = 25M; W4 = 5.7 mm; W6 = 7.01 mm; W8 = 8.10 mm; 1 in. = 25.4 mm; 1 psi = 6.895 kPa.

Several studies have also been conducted on specific reinforcement schemes, performance of the splice between the prestressing strand and deformed steel reinforcing bars,⁹ and design concepts including development of strut-and-tie models.¹⁰

While the design of dapped-end beams typically follows the current *PCI Design Handbook* procedure, field performance remains a concern and dapped-end reinforcement details are not yet standardized within the industry. As such, this study is intended to develop both rational design methodologies for proportioning key reinforcement in dapped-end double tees and standard details that have proved to be effective by extensive analyses and tests. The research findings are reported in two papers: part 1 (this paper), which describes the experimental program under which promising reinforcement schemes and key parameters were tested, and part 2 (a companion paper¹¹), which presents the development of design guidelines for the dapped ends of thin-stemmed members. The research report⁷ provides additional background and research findings on dapped thin-stemmed members, including a literature review, industry experience, the analytical study, and an auxiliary experimental program to study the behavior of the lap splice between the hanger reinforcement tails and pretensioning strand.

Experimental program

The experimental program was developed based on the results of extensive three-dimensional nonlinear finite element models. The testing program consisted of ten 40 ft (12 m) long, dapped-end single-tee beams with different reinforcement schemes for the dapped ends. All beams had a cross section corresponding to one half of a 30 in. (760 mm) deep, 12 ft (3.7 m) wide double tee. **Figure 3** shows the elevation and cross section of the tested specimens. The pretensioning strand pattern and dap dimensions were adjusted for some specimens, but the cross-sectional dimensions remained the same. Each dapped end was tested to failure in a separate test. After testing one end of a beam, the beam was rotated to test the other end. All dapped ends were loaded to several stages of interest, including dead load, service load, and factored design load of a typical 60 ft (18 m) long double-tee beam subjected to both moderate and relatively high uniform loads in a parking structure. The experimental program examined the performance of six different reinforcement schemes and the influence of six parameters that have shown significant behavioral effects based on finite element analyses. **Table 1** summarizes the test matrix of the experimental program. The two ends of each beam are designated by the letters A and B. **Table 1** indicates the parameters and the dap reinforcement used for each specimen. Complete reinforcement details of all 20 tested dapped ends are available in appendix A of the research report.⁷ **Table 2** summarizes the

Table 2. Design loads for test specimens

| Design loads | Load | Service* | Factored [†] |
|--------------|---|----------|-----------------------|
| Moderate | Dead load <i>D</i> , lb/ft ² | 78 | 94 |
| | Live load <i>L</i> , lb/ft ² | 40 | 64 |
| | Snow load <i>S</i> , lb/ft ² | 20 | 10 |
| | Combination, lb/ft ² | 123 | 168 |
| | Vertical dap reaction, kip | 21.9 | 29.5 |
| | Target nominal strength,** kip | | |
| High | Dead load <i>D</i> , lb/ft ² | 78 | 94 |
| | Live load <i>L</i> , lb/ft ² | 80 | 128 |
| | Combination, lb/ft ² | 158 | 222 |
| | Vertical dap reaction, kip | 28 | 40 |
| | Target nominal strength,** kip | | |

Note: 1 lb/ft² = 0.047 kPa; 1 kip = 4.448 kN.

* Service load combination = ($D + 0.75L + 0.75S$) or ($D + L$).

[†] Factored load combination = ($1.2D + 1.60L + 0.50S$) or ($1.2D + 1.6L$).

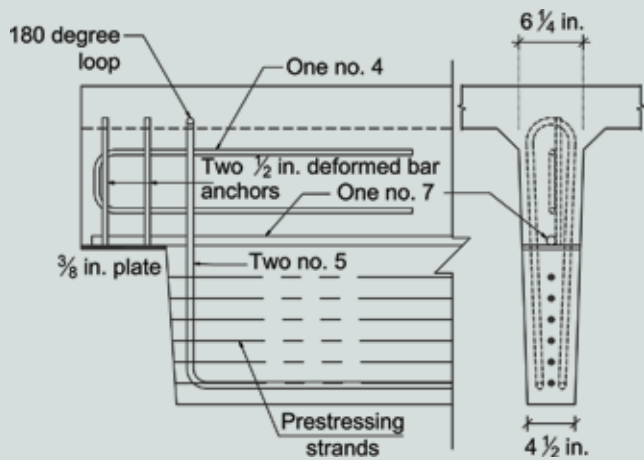
** Target nominal strength is equal to the factored vertical dap reaction divided by the strength reduction factor of 0.75.

design loads for test specimens. The parameters of this experimental program are described in detail in the following sections.

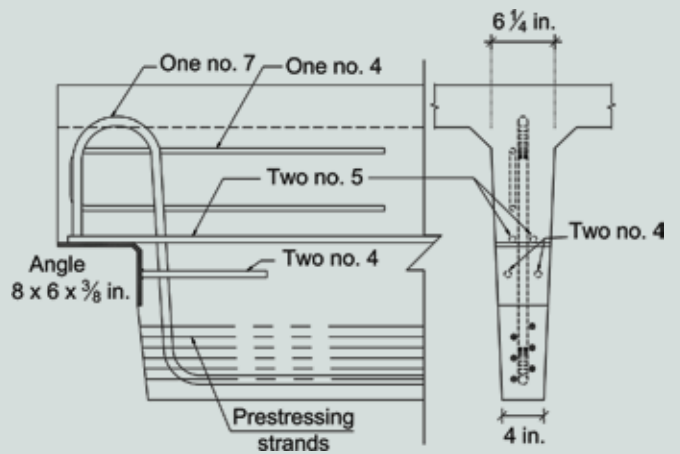
After development of design recommendations based on this experimental program, a 60 ft (18 m) double-tee beam with dapped ends was tested under conditions that closely match those of a parking structure double-tee beam. Four reinforcement schemes were selected for the dapped ends based on results from the primary experimental program. The findings, which are described in the research report,⁷ verified the strength and performance of the full-scale beams.

First parameter: Reinforcement schemes

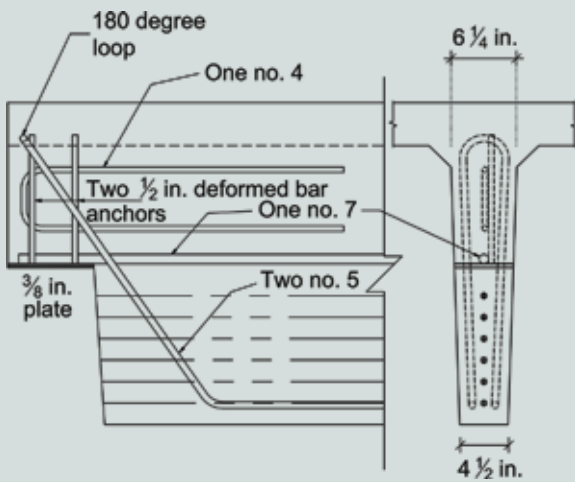
The six reinforcement schemes included in this experimental program were the vertical L scheme, vertical Z scheme, inclined L scheme, vertical C scheme, custom welded-wire reinforcement (WWR) scheme, and CZ scheme. **Figure 4** shows the reinforcement details for each of the six schemes. Dapped-end reinforcement for all six schemes were designed to have the same area of steel for hanger reinforcement and other dapped-end reinforcing steel, allowing for comparison of the performances of the six schemes. For the vertical and inclined L schemes, the beams were prestressed using single-column strand such that the hanger reinforcing bars were located on either side



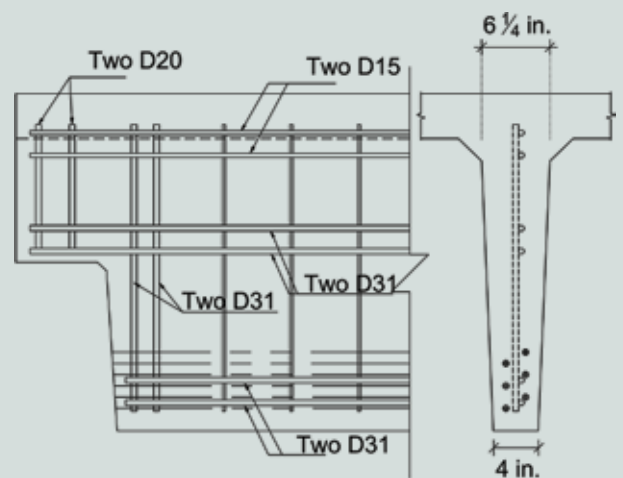
Vertical L scheme (specimen 1A)



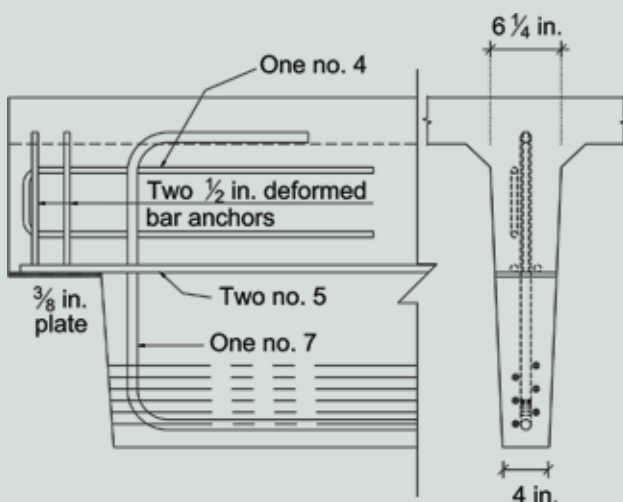
Vertical Z scheme with corner angle (specimen 2A)



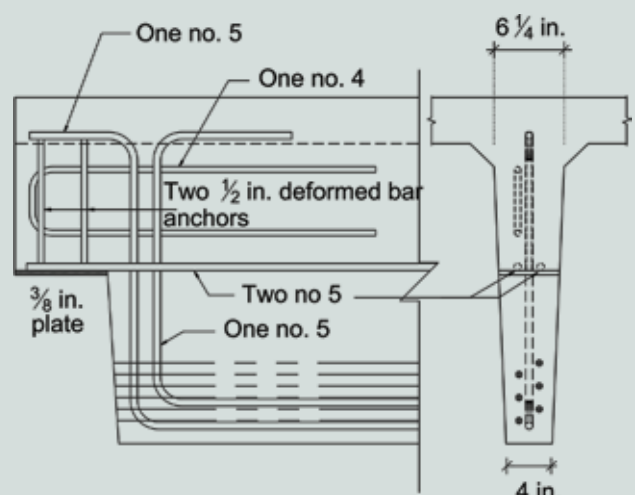
Inclined L scheme (specimen 3A)



Custom welded-wire reinforcement scheme (specimen 4A)



Vertical C scheme (specimen 4B)



CZ scheme (specimen 10A)

Figure 4. Reinforcement details for the six reinforcement schemes. Note: D15 = 11.08 mm; D20 = 12.80 mm; D31 = 15.95 mm; no. 4 = 13M; no. 5 = 16M; no. 7 = 22M; 1 in. = 25.4 mm.

of the strand. For the other schemes—vertical Z, custom WWR, CZ, and vertical C—the beams were prestressed using a staggered arrangement of strands. For the staggered strand arrangement, the hanger reinforcing bars or the WWR were inserted between the strands.

Vertical L scheme Figure 4 shows the details of the vertical L scheme (specimen 1A). The vertical L scheme consisted of two no. 5 (16M) bars provided by one L-shaped reinforcing bar. The L-shaped reinforcing bar was anchored at the top by a 180-degree loop and at the bottom by a bend and horizontal extension that lapped with the bottom strand in the web. The nib flexural reinforcement consisted of one horizontal no. 7 (22M) bar welded to the bearing plate. The shear friction reinforcement in the nib consisted of one no. 4 (13M) horizontal U-shaped reinforcing bar. The diagonal tension reinforcement in the nib consisted of two ½ in. (13 mm) diameter deformed vertical bars welded to the bearing plate.

Vertical Z scheme Figure 4 shows details of the vertical Z scheme (specimen 2A). In some of the vertical Z specimens, the bearing plate at the beam end was replaced with a steel angle, referred to as the corner angle (Fig. 4). The corner angle detail was used to better control cracking at the reentrant corner. In this detail, the hanger and flexural steel are welded to the angle. The vertical Z scheme consisted of one no. 7 (22M) Z-shaped reinforcing bar anchored at its upper end by a 180-degree bend and welded to the bearing plate or corner angle. The lower end of the Z-shaped bar was anchored by extending the bar along the bottom of the stem. The nib flexural reinforcement consisted of two no. 5 (16M) reinforcing bars welded to the bearing plate or horizontal leg of the corner angle. The nib diagonal tension reinforcement was provided by the vertical leg of the hanger steel in the nib that was welded to the bearing plate or corner angle. Shear friction reinforcement of the nib was provided by one no. 4 (13M) horizontal U-shaped bar. Two ½ in. (13 mm) diameter deformed bar anchors were used to anchor the vertical leg of the angle to the concrete. This reinforcement scheme provides an important advantage in reducing the reinforcement congestion in the nib, thus providing better placement and compaction of concrete within the nib.

Inclined L scheme Figure 4 shows details of the inclined L scheme (specimen 3A). The inclined L scheme is similar to the vertical L scheme except for the orientation of the hanger reinforcement bars, which were inclined at an angle of 55 degrees to the horizontal.

Custom WWR scheme This reinforcement scheme consists of a single custom WWR grid (specimen 4A). The reinforcement grid is prefabricated and placed as one unit, thus expediting the reinforcement placing process and minimizing errors. Figure 4 shows the reinforcement details for the custom WWR scheme. The hanger steel consisted

of two vertical deformed D31 (15.9 mm) wires anchored at the top and bottom by welding to crossbars. The nib flexural reinforcement and shear friction reinforcement consisted of two D31 wires, and the nib diagonal tension reinforcement consisted of two D20 (12.8 mm) wires. W4 (5.7 mm) wires spaced at 6 in. (150 mm) served as the shear reinforcement for the full-depth section.

Vertical C scheme The vertical C scheme is widely used in the precast concrete industry. Figure 4 shows the dapped-end reinforcement details for the vertical C scheme (specimen 4B). The hanger steel consisted of one no. 7 (22M) C-shaped bar. The upper end of the bar was anchored by extending the bar to the full depth of the section along the web-flange junction, while the lower end was extended along the bottom of the web to lap with the prestressing strand. Shear friction reinforcement of the nib consisted of one no. 4 (13M) U-shaped reinforcing bar. The diagonal tension reinforcement of the nib consisted of two ½ in. (13 mm) diameter deformed vertical bars welded to the bearing plate.

CZ scheme The CZ scheme combines the Z and C schemes. Figure 4 shows details of the CZ scheme (specimen 10A). The hanger reinforcement for this scheme is composed of one no. 5 (16M) C-shaped bar and one no. 5 Z-shaped bar. The upper end of the C-shaped bar was turned toward the full-depth section, while the upper end of the Z-shaped bar was turned toward the nib. The lower ends for both bars were extended along the bottom of the stem and lapped with the pretensioned strand. The nib flexural reinforcement consisted of two no. 5 bars welded to the end plate. Shear friction reinforcement of the nib was provided by one no. 4 (13M) U-shaped reinforcing bar, and the nib diagonal tension reinforcement consisted of two ½ in. (13 mm) diameter deformed vertical bars welded to the bearing plate.

Second parameter: Hanger reinforcement and stem reinforcement

The tested beams were designed using typical loads acting on a 60 ft (18 m) double-tee beam typically used for parking structures. Two different load levels were considered in the design. The first load level corresponded to moderate loads representing those typically used for parking structures; the second load level corresponded to high loads, such as may be encountered in heavy snow regions or where double tees support landscaping or storage loads. For the first three beams in Table 1, ends designated by the letter A were designed using moderate loads, while ends designated by the letter B were designed using high loads. Accordingly, the hanger and shear reinforcement in end A was proportioned for moderate loads, and these reinforcement quantities were increased for the higher demand in end B.

Table 3. Summary of failure loads and failure modes for all tested beams

| Specimen | f'_c on day of test, psi | Vertical dap reaction at failure, kip | Vertical dap reaction at factored load, kip | Maximum crack width at service load,* in. | Failure mode |
|----------|----------------------------|---------------------------------------|---|---|---|
| 1A | 6970 | 42.8 | 29.5 | 0.015 | Concrete crushing in the bottom corner |
| 1B | 6970 | 52.7 | 40.0 | 0.015 | Flexure-shear after splitting and strand slip |
| 2A | 8450 | 51.2 | 29.5 | 0.005 | Diagonal tension cracking in the web |
| 2B | 8450 | 59.3 | 40.0 | 0.015 | Diagonal tension cracking in the web |
| 3A | 7400 | 50.2 | 29.5 | 0.005 | Diagonal tension cracking in the web |
| 3B | 7400 | 53.8 | 40.0 | 0.010 | Flexure-shear after splitting and strand slip |
| 4A | 8450 | 40.0 | 29.5 | 0.020 | Diagonal tension cracking in the web |
| 4B | 8450 | 45.9 | 29.5 | 0.015 | Diagonal tension cracking within the nib |
| 5A | 8340 | 55.3 | 29.5 | 0.005 | Diagonal tension cracking in the web |
| 5B | 8340 | 67.4 | 40.0 | 0.005 | Diagonal tension cracking in the web |
| 6A | 12,767 | 59.6 | 40.0 | 0.015 | Flexure shear after splitting and strand slip |
| 6B | 12,767 | 59.2 | 40.0 | 0.010 | Concrete crushing in the bottom corner |
| 7A | 7650 | 43.4 | 40.0 | 0.020 | Diagonal tension cracking in the web |
| 7B | 7650 | 52.7 | 40.0 | 0.015 | Diagonal tension cracking within the nib |
| 8A | 8650 | 44.3 | 29.5 | 0.015 | Diagonal tension cracking within the nib |
| 8B | 8650 | 44.6 | 29.5 | 0.005 | Diagonal tension cracking in the web of the reduced section |
| 9A | 8100 | 51.0 | 29.5 | 0.015 | Concrete crushing in the bottom corner |
| 9B | 8100 | 38.6 | 29.5 | 0.015 | Flexure shear after splitting and strand slip |
| 10A | 8340 | 49.1 | 29.5 | 0.010 | Diagonal tension cracking in the web |
| 10B | 8340 | 31.5 | 29.5 | 0.015 | Diagonal tension cracking within the nib |

Note: f'_c = compressive strength of concrete. 1 in. = 25.4 mm; 1 kip = 4.448 kN; 1 psi = 6.895 kPa.

* Vertical dap reaction at service load for moderate-load specimens is 21.9 kip and for high-load specimens is 28.0 kip.

Third parameter: Prestressing the nib

To study the effect of prestressing the nib, specimens 2B and 5B were identical in all aspects except that specimen 5B had two strands passing through the nib. Prestressing the nib is expected to enhance shear strength and reduce cracking at the reentrant corner and in the full-depth section of the beam.

Fourth parameter: Concrete strength

The effect of the concrete strength on the behavior was investigated by comparing the behavior of specimens 1B and 6B with design concrete

strengths of 6000 and 10,000 psi (41 and 69 MPa), respectively. On the day of testing, the actual concrete strengths were significantly higher than these values (Table 3).

Fifth parameter: Shear reinforcement of the web

To study the effect of high amounts of shear reinforcement within the web, specimen 7B, which was reinforced with heavier stem reinforcement (W8 [8.1 mm] at 4 in. [100 mm] spacing), was compared with specimen 4B, which was reinforced with lighter stem reinforcement (W4 [5.7 mm] at 6 in. [150 mm] spacing).

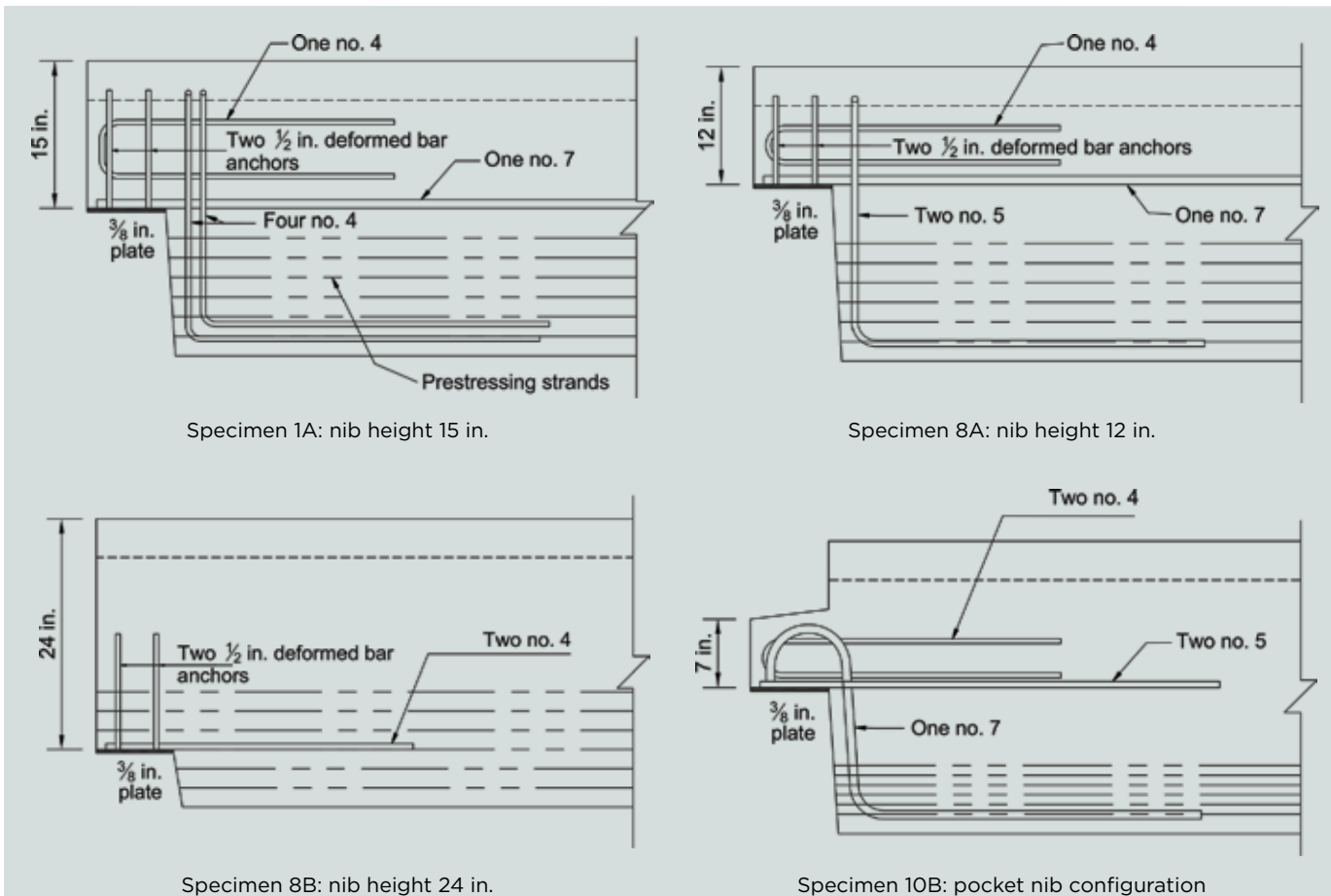


Figure 5. Specimens 1A, 8A, and 8B with different nib heights and specimen 10B with pocket nib configuration. Note: no. 4 = 13M; no. 5 = 16M; no. 7 = 22M; 1 in. = 25.4 mm.

Sixth parameter: Nib height and configuration

Three specimens with different nib heights were tested to study the effect of the height of the nib on strength and mode of failure. The three nib heights used in this study were 12, 15, and 24 in. (300, 380, and 610 mm) (Fig. 5). The selected heights were 40%, 50%, and 80% of the full height of the beam, respectively. The hanger reinforcement and nib shear friction reinforcement were omitted for specimen 8B with the 24 in. nib height. The reinforcement details for specimen 8B were designed to examine the possibility of omission of the dapped-end reinforcement for dap height (notch) less than or equal to 20% of the full member height.

Specimen 10B was configured to test the extreme condition where the nib is further reduced to fit into a pocket spandrel to determine whether such a configuration is viable (Fig. 5).

Seventh parameter: Splice length of the hanger reinforcement

To examine the effect of the splice length on the behavior, specimens 9B, 1A, and 9A were designed to have

different splice lengths of 15, 36, and 60 in. (380, 910, and 1500 mm), which correspond respectively to 0.94, 2, and 3.75 times the development length of the no. 5 (16M) hanger steel bar calculated in accordance with the American Concrete Institute's (ACI's) *Building Code Requirements for Structural Concrete (ACI 318-14)* and *Commentary (ACI 318R-14)*.¹² Figure 6 shows the three splice length details.

Test setup and instrumentation

All tested dapped ends were supported by a pin link and were loaded to failure using hydraulic jacks close to the dapped end being tested. Figure 7 shows an isometric view of the test setup. The inclined link support (Fig. 8) was used at the tested end to maintain a horizontal reaction as a percentage of the vertical reaction and to allow end rotation. This horizontal reaction was resisted at the other end of the beam by a pin connection. The link support was inclined at an 11-degree angle with respect to the vertical plane to produce a horizontal reaction equal to 20% of the vertical reaction, as recommended by the *PCI Design Handbook*.

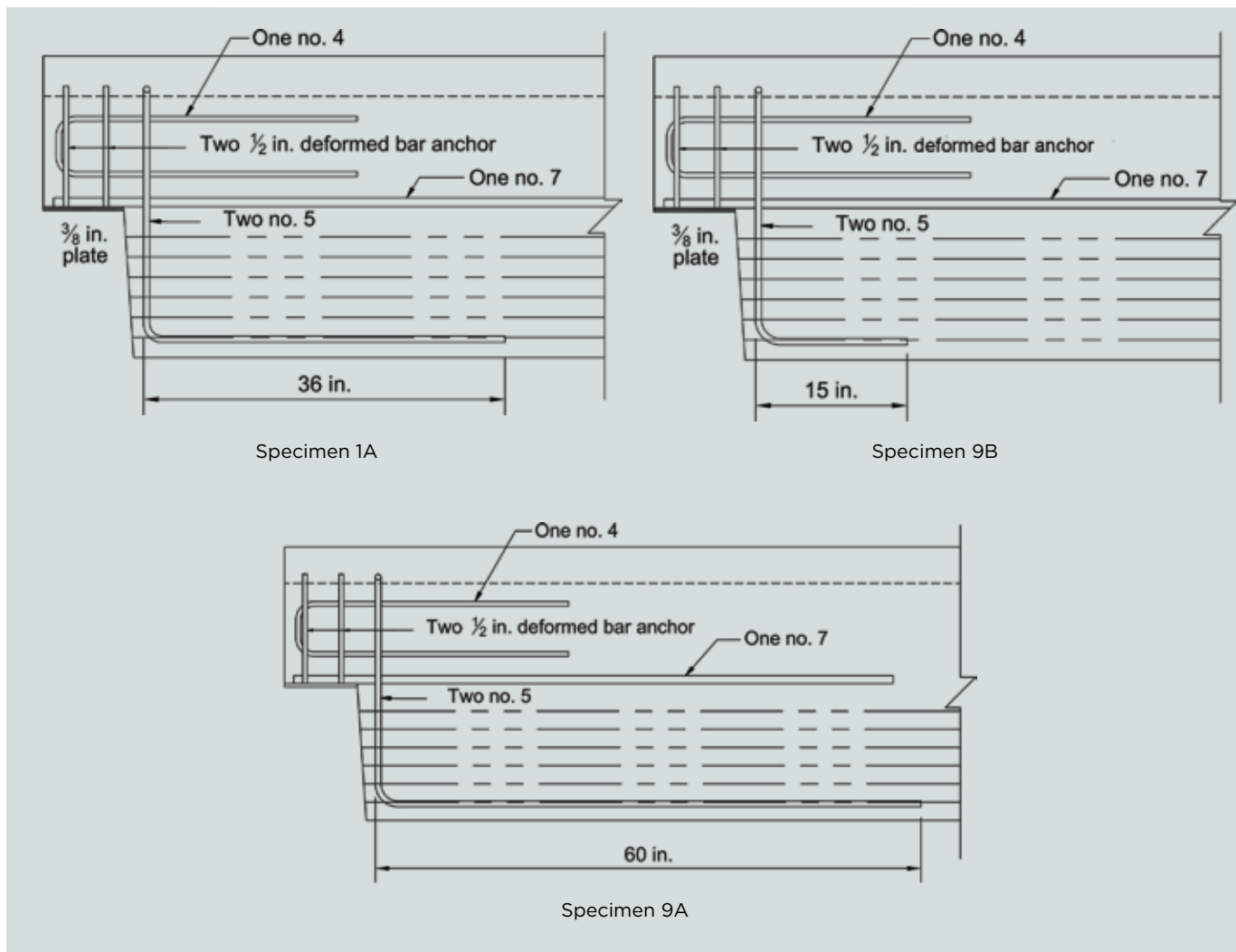


Figure 6. Specimens 1A, 9B, and 9A with different splice lengths. Note: no. 4 = 13M; no. 5 = 16M; no. 7 = 22M; 1 in. = 25.4 mm.

The steel pin at the top of the inclined link was welded to the bearing plate cast into the nib of each beam. The middle of the steel pin was milled flat so that the bearing plate would sit level on the pin and provide a large area to weld. The top pin was allowed to rotate within the link, and the link itself was allowed to rotate about its base so that the beam could deform freely in the horizontal direction and rotate about the top pin. After the conclusion of each test, the pin was cut away from the bearing plate and the inclined link setup was reused for all tested beams.

Load was applied to the specimen by four hydraulic jacks (Fig. 8). All four hydraulic jacks shared the same pressure source, ensuring equally applied loads. The jacks were operated manually with an electric pump to apply load incrementally to failure. The four hydraulic jacks were connected to two loading beams located across the top of the specimen, placed 7 and 10 ft (2 and 3 m) from the end of the beam.

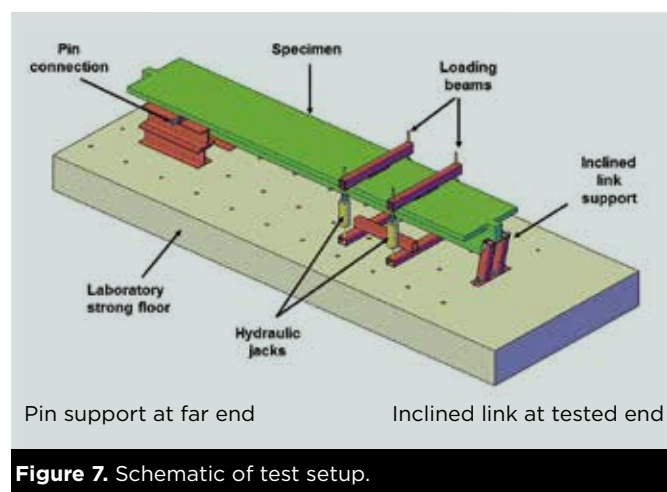


Figure 7. Schematic of test setup.

The performance, including end deflections, strain, and applied loads, was monitored at service and factored load levels according to the loads specified in Table 2. Crack patterns and crack width measurements were recorded for



General view



Inclined link support

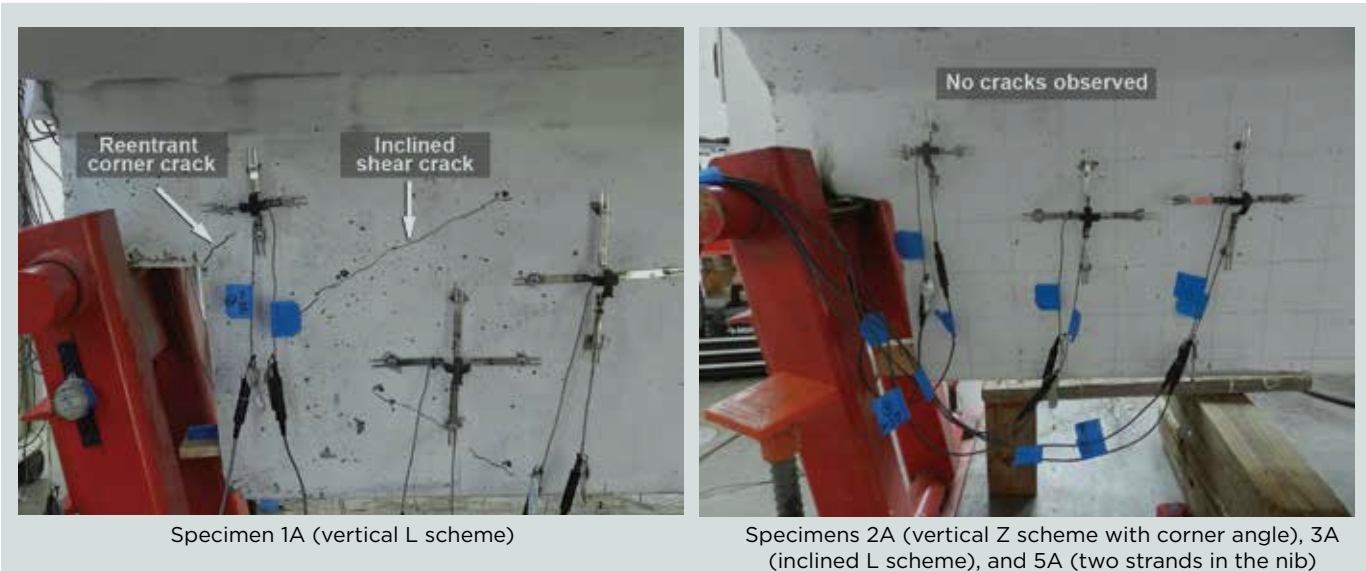
each load level. The vertical reaction of each tested dap was monitored throughout testing.

The applied loads were measured using load cells placed at two opposite loading points. String potentiometers were used to measure the deflection at four selected points along the specimen. Slip of the bottom prestressing strand was monitored using a displacement sensor installed on the strand on the end face of the specimen. Weldable strain gauges were installed at various locations on the steel reinforcement before the casting of each specimen. Concrete strain measurements were taken using strain gauges with gauge lengths of 4 and 8 in. (100 and 200 mm). Three orthogonal pairs of strain gauges were applied to one face of the dapped end. The first pair of strain gauges was positioned close to the reentrant corner to capture strains resulting from the reentrant corner cracks. The second and third pairs were positioned in the full-depth section to capture strains resulting from diagonal cracks in the web.

Test results

Table 3 gives a summary of test results for all tested beams. The observed failure mode for each beam is given along with the maximum vertical reaction measured at failure for each dapped end. The factored vertical dap reaction ($1.2D + 1.6L + 0.5S$, where D is the dead load, L is the live load, and S is the snow load) for each dapped end based on a full-scale 60 ft (18 m) long beam is listed as well. In general, the measured failure load was always greater than the required strength based on the factored design loads. Table 3 also lists the measured concrete strength determined on the day of testing for each specimen, as well as the maximum measured crack width at service load for each specimen. Record-

Figure 8. Test setup.



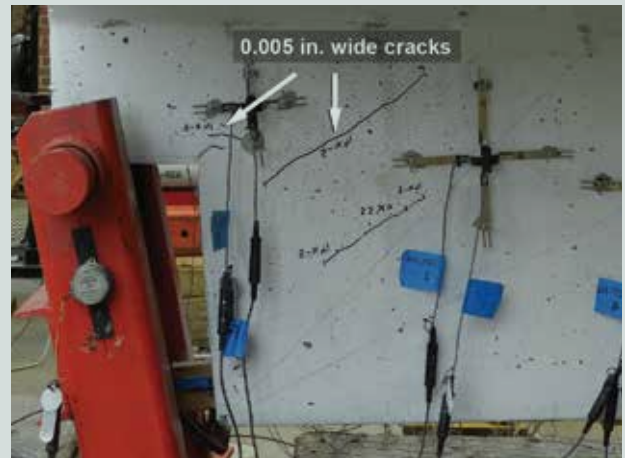
Specimen 1A (vertical L scheme)

Specimens 2A (vertical Z scheme with corner angle), 3A (inclined L scheme), and 5A (two strands in the nib)

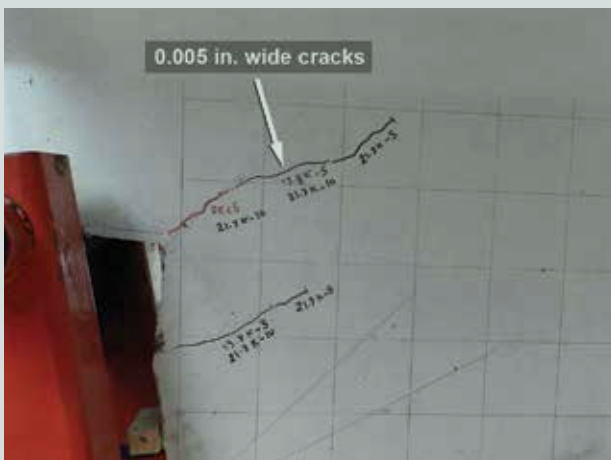
Figure 9. Preexisting cracks before loading for selected specimens.



Specimen 1A (vertical L scheme)



Specimen 3A (inclined L scheme)



Specimen 2A (vertical Z scheme with corner angle)



Specimen 5A (two strands in the nib)

Figure 10. Crack patterns at service load for selected specimens. Note: 1 in. = 25.4 mm.

ed data for each of the 20 dapped-end specimens, including detailed descriptions of the behavior at various load levels, photos of the crack patterns at various load levels, load-deflection plots, and load-strain plots are available in appendix B of the research report.⁷

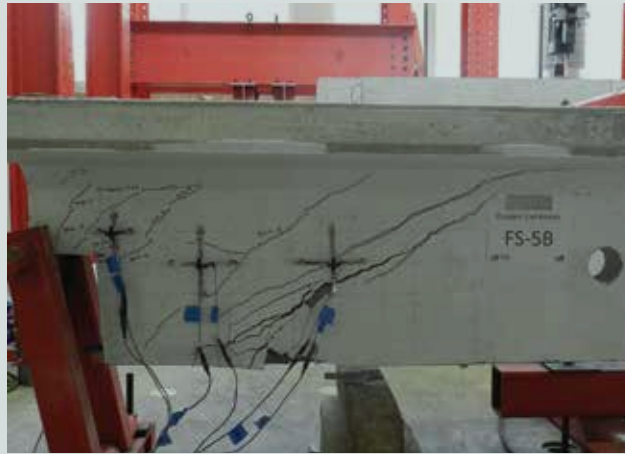
Preexisting cracks before loading

In some of the test specimens, inclined hairline cracks were observed on web faces before testing. These cracks generally initiated at the reentrant corner and extended upward toward the web-flange junction at an angle of approximately 45 degrees to the horizontal. The length of the reentrant corner crack varied between specimens owing to different arrangements of reinforcement used for the dapped ends. In addition to the reentrant corner cracks, other inclined shear cracks were also visible in the full-depth section for some specimens. All of these initial cracks were generally narrow, with crack widths less than 0.005 in. (0.13 mm). In some reinforcement schemes, cracks were not observed

before loading, including the inclined L and the vertical Z with corner angle. Preexisting cracks were not observed in the specimens with strands passing through the nib. **Figure 9** shows examples of cracks observed before loading for some selected specimens.

Crack patterns at service load

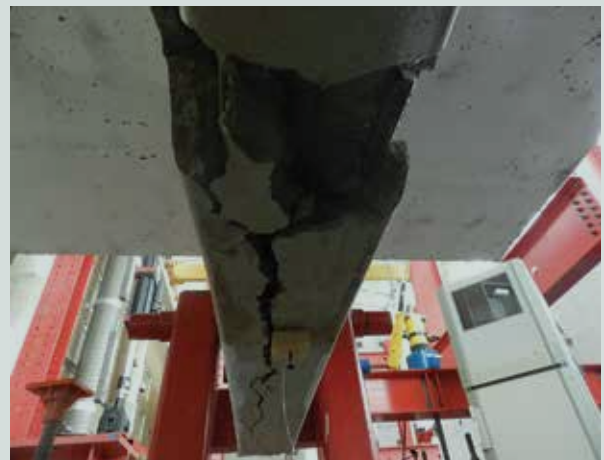
As the load was increased to service load level, preexisting reentrant corner cracks extended toward the web-flange junction at an angle of approximately 45 degrees. Also, in some specimens, the inclined shear cracks in the full-depth section extended to the web-flange junction and downward toward the face of the dap. For the majority of the specimens, cracking was localized near the reentrant corner and in the region of the full-depth section adjacent to the reentrant corner. Most of these cracks extended all the way to the web-flange junction. No major diagonal tension cracks were observed in the full-depth section away from the



Diagonal tension cracking in the web



Flexure-shear failure



Associated splitting in the web



Diagonal tension cracking within the nib



Concrete crushing at the bottom corner

Figure 11. Failure modes for the dapped ends.

reentrant corner at service load level. The extent of cracking and crack widths varied from one specimen to the other according to the amount and arrangement of the reinforcement at the dapped end. The maximum

measured crack width at service load varied from 0.005 to 0.02 in. (0.13 to 0.5 mm) for all tested specimens. **Figure 10** shows typical cracking observed at the service load level for selected specimens. The cracking

patterns observed at service load indicated that the vertical Z with corner angle and the inclined L reinforcement schemes exhibited the best performance in terms of crack control compared with all other schemes. For the inclined L scheme, the orientation of the hanger steel normal to the diagonal tension cracks effectively arrested the cracks at service loads. For the vertical Z scheme, use of the corner angle effectively reduced cracking at service load. No cracks were observed at service load for the specimens with strands in the nib because prestressing the nib applies direct precompression force to the concrete section in the nib region and the full-depth section, which prevented formation of cracks up to the service load level.

Failure modes

Nine of the 20 dapped ends failed due to the formation and widening of a critical diagonal tension crack within the web. This diagonal tension crack extended from or close to the bottom corner of the web up to the web flange junction with an angle of inclination of 30 to 45 degrees from the horizontal. In some cases, the diagonal tension crack occurred so abruptly that it was not possible to specify its origin and the load dropped significantly upon the formation of this crack. In other cases, usually for specimens with webs that had higher amounts of stem reinforcement, a series of diagonal tension cracks occurred in the web before the formation of the critical crack that caused ultimate failure. Although the final failure was brittle, this type of failure was preceded by extensive cracking near the reentrant corner and dap end face before the critical diagonal crack took place. Strand slip measurements indicated significant slip that occurred immediately after the initiation of the critical diagonal tension crack. This observation indicates strand bond failure, which implies that the tension chord of the beam was effectively disabled after the formation of the critical diagonal crack. **Figure 11** shows the typical diagonal tension failure in the web.

Four of the twenty dapped ends failed due to flexure-shear cracking at the bottom of the web in the region where the horizontal extension of the hanger steel terminated. Before failure, a longitudinal splitting crack developed along the bottom of the web. This splitting crack extended from the dap to the end of the horizontal extension of the hanger reinforcement. The flexure-shear crack occurred shortly after longitudinal splitting of the web. Thus, the flexural shear crack resulted from the strand bond failure caused by the longitudinal splitting of the web. Figure 11 shows the flexure-shear failure after splitting of the web. This failure mode was observed in specimens 1B and 3B with four no. 4 (13M) hanger reinforcing bars. After failure, the concrete was removed and the reinforcing bars were exposed. Removing the concrete revealed improper placement of the hanger bars, which resulted in side and bottom covers less

| Reinforcement scheme | Strand pattern | | Performance | | |
|----------------------|----------------|-----------------------|-------------|----------------|------------------|
| | 1 column | Staggered or 2 column | Strength | Serviceability | Constructability |
| Vertical L | ■ | ■ | ● | ● | ● |
| Vertical C | ■ | ■ | ● | ● | ● |
| Inclined L | ■ | ■ | ● | ● | ● |
| Vertical Z | ■ | ■ | ● | ● | ● |
| Customized WWR | ■ | ■ | ● | ● | ● |
| Vertical CZ | ■ | ■ | ● | ● | ● |

| Performance legend | |
|--------------------|------|
| ● | Best |
| ● | Good |
| ● | Fair |

| Strand pattern legend | |
|-----------------------|---|
| ■ | Use single hanger reinforcing bar between strand columns |
| ■ | Use two layers of hanger reinforcement on either side of strand column. |
| ■ | Cannot be placed |
| ■ | Use two layers of WWR on either side of single strand column or one layer of WWR between two strand columns |

Figure 12. Reinforcement scheme performance summary. Note: WWR = welded-wire reinforcement.

than permitted by ACI 318-14. The premature splitting in the web was presumably due to inadequate confinement at bars with shallow covers. Specimen 6A, with two no. 6 (19M) bars as hanger reinforcement, also failed in this mode. This can be attributed to the use of large-diameter no. 6 bars in the tight webs, which increased the potential for splitting failure due to the reduction of the concrete effective area surrounding the bars and high splitting forces generated due to bar development and dilation of the prestressing strands (Hoyer effect).

The third failure mode for the dapped ends was due to diagonal tension cracking within the nib. The critical

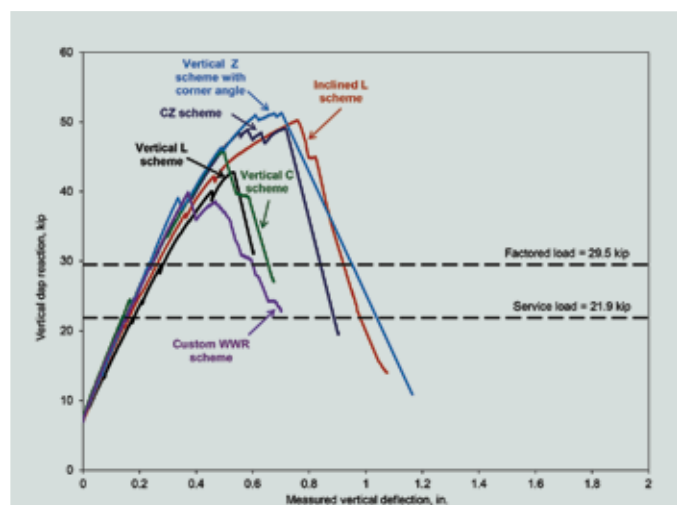


Figure 13. Measured vertical deflections for the six reinforcement schemes. Note: WWR = welded-wire reinforcement. 1 in. = 25.4 mm; 1 kip = 4.448 kN.

Research findings

Based on the results observed from the experimental program, the effects of various parameters on dapped-end behavior are described in the following sections.

First parameter: Reinforcement schemes

All six reinforcement schemes achieved ultimate capacities significantly higher than their factored design load and were sufficient to ensure that failure modes outside the dapped-end region would control. However, actual concrete strength exceeding the design strength contributed to the ultimate capacity of these specimens. **Figure 12** compares the constructibility and performance characteristics of the reinforcement schemes considered in this research.

The factored design load, based on $1.2D + 1.6L + 0.5S$, was 29.5 kip (131 kN) for all six beams. **Figure 13** plots the measured load deflection at the location of the applied load for the six reinforcement schemes. The two reinforcement schemes with the best performance with respect to ultimate capacity were those with the vertical Z with corner angle and the inclined L. The reinforcement scheme with the lowest ultimate strength performance was the custom WWR. The CZ, vertical C, and vertical L schemes performed well, with ultimate capacities substantially exceeding factored loads. All reinforcement schemes failed due to diagonal tension cracking in the web except for the vertical C scheme, which failed due to diagonal cracking in the nib. Table 3 gives the measured vertical dap reactions at failure for the six reinforcement schemes.

Figure 14 plots the crack width versus the dap reaction for the six reinforcement schemes. **Figure 15** shows a summary of the maximum crack widths at a service load level of 21.9 kip (97.4 kN) for each reinforcement scheme. Comparison of crack widths with the dap vertical reactions for the six reinforcing schemes indicated that the vertical Z with corner angle and the inclined L schemes exhibited the best performances in terms of crack control. The reentrant corner crack width for these two schemes was less than 0.005 in. (0.13 mm) at service load. The custom WWR scheme had the widest crack, with a width of 0.02 in. (0.50 mm) at service load. The vertical L, vertical C, and CZ schemes showed good performance, with crack widths ranging from 0.010 to 0.015 in. (0.25 to 0.38 mm) at service load.

The superior performance of the vertical Z scheme with corner angle can be attributed to the use of the corner angle, which effectively reduced cracks at service load by resisting the cantilever bending of the nib section and providing a rigid connection between the nib section and the full-depth section at the reentrant corner location. Furthermore, welding the vertical Z-shaped hanger bar

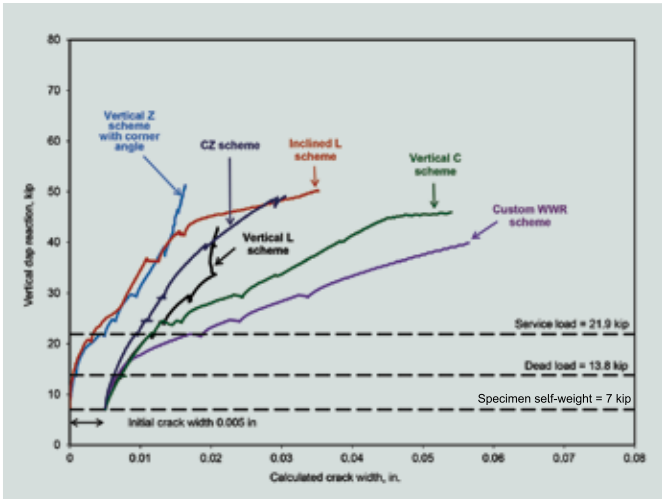


Figure 14. Reentrant corner crack width for six reinforcement schemes (calculated from strain data). Note: WWR = welded-wire reinforcement. 1 in. = 25.4 mm; 1 kip = 4.448 kN.

diagonal crack started from the inside edge of the bearing pin and extended upward to the web-flange junction. Specimens 8A and 10B, with reduced nib heights, failed in this mode. Specimens 4B and 7B, both with the typical nib height of 15 in. (380 mm) and vertical C scheme, also failed in this mode. Diagonal tension cracks in the nib region extending up from the bearing are not captured by the C-hanger reinforcing bar detail because the upper end of the bar is anchored by turning it toward the full-depth section rather than out toward the nib. The diagonal tension crack in the nib extended upward and ran around the upper bend region of the C-shaped bar. Figure 11 shows the diagonal tension cracking within the nib.

The last failure mode observed in the dapped ends was a sudden diagonal compression crushing of the concrete at the bottom corner of the web (Fig. 11). This failure mode was brittle and sudden in nature. Specimens 1A, 6B, and 9A failed in this mode.

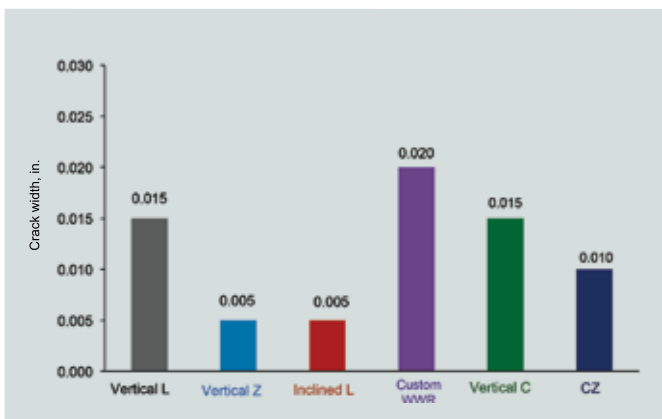


Figure 15. Crack widths at service load level (21.9 kip [97.4 kN]) for six reinforcement schemes. Note: WWR = welded-wire reinforcement. 1 in. = 25.4 mm.

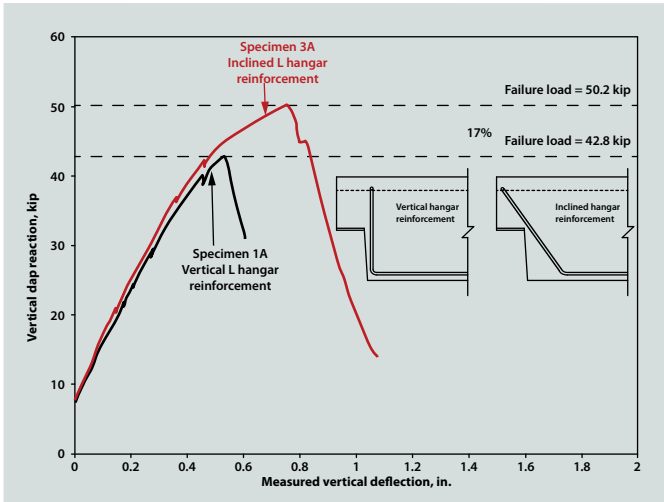


Figure 16. Measured vertical deflections for specimens 1A (vertical hanger bars) and 3A (inclined hanger bars). Note: 1 in. = 25.4 mm; 1 kip = 4.448 kN.

to the corner angle provided positive anchorage for the hanger reinforcement. The inclined L scheme also showed excellent performance with respect to ultimate strength and crack control at service load. This can be attributed to the orientation of the hanger steel normal to the diagonal tension cracks, which effectively arrested the cracks at service loads. Good anchorage of the hanger steel through a 180 degree loop at the upper end of the bar enabled the bar to develop its yield strength before failure. This was evidenced by the measurements of the strain gauge installed on the hanger bar, indicating yielding of the reinforcing bar before failure.

The CZ scheme exhibited good performance compared with its counterparts. This scheme provides an important advantage due to ease of its construction and good anchorage of the hanger bars in the compression zone in the beam. The vertical L and vertical C schemes showed moderate performance compared with other schemes. The C-shaped bar did not arrest the diagonal tension crack of the nib region because the upper end of the bar is turned in toward the full-depth section rather than out toward the nib section.

The custom WWR scheme showed the worst performance of all schemes in terms of ultimate capacity and crack control at service load. Unlike all of the other schemes, this scheme had no end bearing plate, which resulted in poor anchorage of the WWR because it was not welded to the end plate. In addition, eccentric placement of the WWR resulted in wider cracks on one face of the dapped end compared with the opposite face.

The effect of the orientation of the hanger reinforcing bars was studied by comparing specimen 1A, which had vertical L hanger bars, with specimen 3A, which

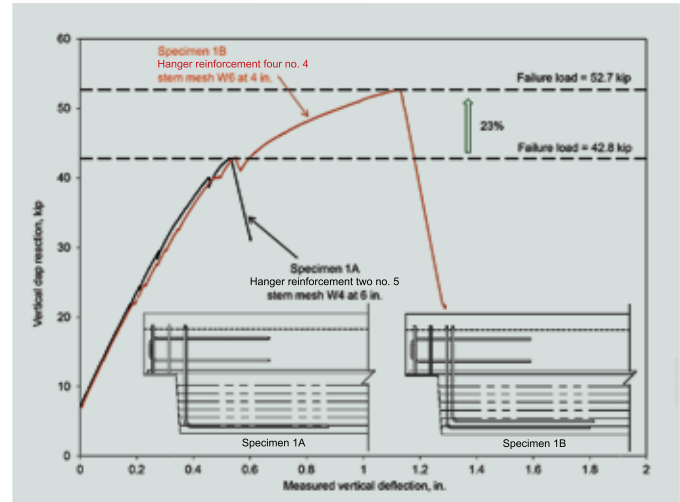


Figure 17. Measured vertical deflections for specimens 1A and 1B. Note: no. 4 = 13M; no. 5 = 16M; W4 = 5.7 mm; W6 = 7.01 mm; 1 in. = 25.4 mm; 1 kip = 4.448 kN.

had inclined L hanger bars. **Figure 16** plots the vertical deflections versus measured loads for specimens 1A and 3A. The inclined L scheme exhibited a 17% increase in ultimate strength and much greater deflection before failure compared with the vertical L scheme. The improved performance of the inclined orientation compared with vertical orientation can be attributed to the angle of the hanger reinforcement, which is nearly parallel to the diagonal tension field.

Second parameter: Hanger reinforcement and stem reinforcement

The effect of the amount of the hanger reinforcement and stem WWR was investigated by comparing the behavior of specimens 1A and 1B, which were designed using moderate level and high level loads, respectively. Specimen 1A was designed to have two no. 5 (16M) bars as hanger reinforcement and W4 (5.7 mm) at 6 in. (150 mm) spacing as stem WWR, while specimen 1B was designed to have four no. 4 (13M) hanger bars and W6 (7.0 mm) at 4 in. (100 mm) spacing as stem WWR. **Figure 17** compares the measured vertical deflections under the load for specimens 1A and 1B. Figure 17 highlights the effect of increasing the hanger reinforcement and the stem WWR on the strength and ductility of a dapped end. While specimen 1A failed abruptly after the formation of a diagonal tension crack in the web, specimen 1B, with a higher amount of hanger steel and stem WWR, sustained 23% more load and considerably more deflection before ultimate failure.

Third parameter: Nib prestressing

The effect of this parameter was investigated by comparing specimens 2B and 5B, which are identical except that specimen 5B had two strands passing through the

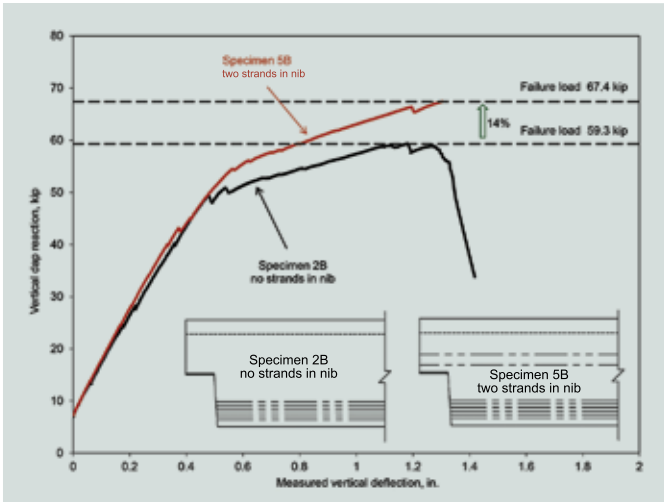


Figure 18. Measured vertical deflections for specimens 2B and 5B. Note: 1 in. = 25.4 mm; 1 kip = 4.448 kN.

nib. **Figure 18** compares the measured load with vertical deflections for specimens 2B and 5B. The results indicated a 14% increase in the ultimate strength for the case where two prestressing strands were located in the nib. This is attributed to the fact that having prestressing strands in the nib applies direct compression force to the concrete section in the nib region and the full-depth section of the beam. Prestressing of the nib also helps delay the formation of the reentrant corner crack and increases the shear strength of the full-depth section. It prevented cracking before loading and limited the width of the reentrant corner cracks at service loads. Specimen 5B with strands in the nib exhibited narrow reentrant corner cracks at service loads, whereas the identical specimen 2B without nib prestressing exhibited approximately 0.015 in. (0.38 mm) wide cracks at the service load level.

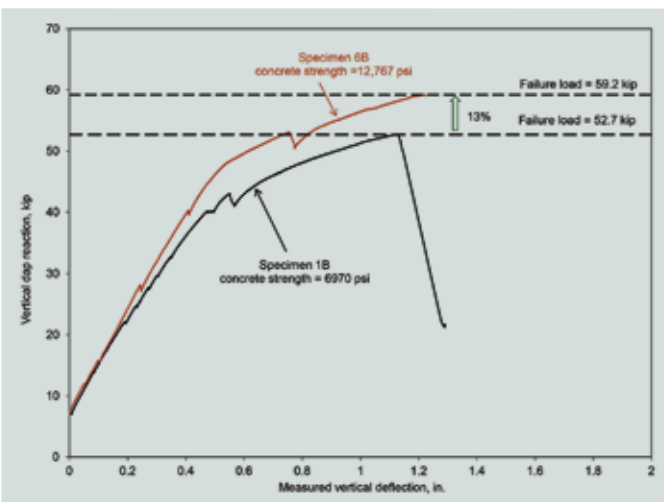


Figure 19. Measured vertical deflections for specimens 1B and 6B. Note: 1 in. = 25.4 mm; 1 kip = 4.448 kN; 1 psi = 6.895 kPa.

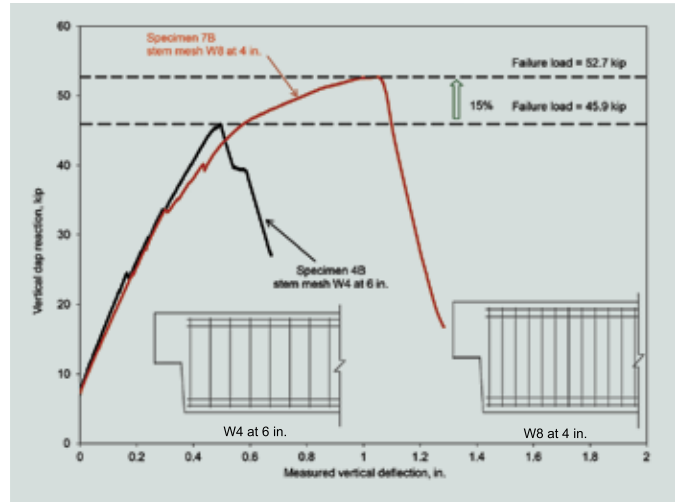


Figure 20. Measured vertical deflections for specimens 4B and 7B. Note: W4 = 5.7 mm; W8 = 8.10 mm; 1 in. = 25.4 mm; 1 kip = 4.448 kN.

Fourth parameter: Concrete strength

The effect of this parameter was investigated by comparing specimens 1B and 6B with measured concrete strengths on the day of testing of 6,970 and 12,767 psi (48.10 and 88.028 MPa), respectively. **Figure 19** compares the measured load with vertical deflections for specimens 1B and 6B. The results indicated a 13% increase in the ultimate strength for the beam with the higher concrete strength. The ratio of the square root of the concrete strength of specimen 6B to that of specimen 1B was 1.35. This indicates that the increase in strength was not directly proportional to the square root of the concrete strength, which is reasonable because reinforcement also contributes to strength and the contribution of concrete strengths in excess of 10,000 psi (69 MPa) is questionable. Although the concrete strength was the only variable between these two specimens, the two specimens failed in different modes. Specimen 1B failed due to flexure-shear cracking, while specimen 6B failed due to concrete crushing in the bottom corner of the web. Both specimens exhibited similar crack patterns and widths under service load, indicating that concrete strength did not significantly affect crack control in these specimens.

Fifth parameter: Shear reinforcement of the web

The effect of increasing both hanger reinforcement and vertical shear reinforcement is discussed under Second Parameter: Hanger Reinforcement and Stem Reinforcement. The effect of the amount of vertical shear reinforcement in the web outside of the nib region (without increasing hanger reinforcement) can be investigated by comparing specimens 4B and 7B. Specimen 7B was designed to have W8 (8.1 mm) at 4 in. (100 mm) spacing as stem reinforcement, whereas specimen 4B had W4 (5.7 mm) at



Specimen 1A (15 in. nib height)



Specimen 8A (12 in. nib height)



Specimen 8B (24 in. nib height)

Figure 21. Specimens after failure. Note: 1 in. = 25.4 mm.

6 in. (150 mm) spacing. **Figure 20** compares the measured load with vertical deflections for specimens 4B and 7B. Specimen 7B exhibited a 15% increase in ultimate strength compared with specimen 4B. Although specimens 4B and 7B both failed due to diagonal tension cracking in the nib, a significant difference in the behavior was observed between the two specimens. Specimen 7B, with the heavier stem WWR, exhibited excessive diagonal cracking in the web before failure. A series of diagonal tension cracks evenly distributed took place in the web as the load was increased up to failure. However, specimen 4B showed a rather brittle and sudden failure without warning. The increase in stem WWR allowed significant cracking in the full-depth section, postcracking strength gain, and considerably more deflection before failure.

No significant effect from increasing the stem WWR was observed for the reentrant corner cracking. This behavior is expected because the stem WWR arrests the diagonal tension cracks in the web rather than the reentrant corner

cracks, which are often controlled by the hanger steel close to this location.

Sixth parameter: Nib height and configuration

The effect of this parameter was investigated by comparing specimen 8A, with a nib height of 12 in. (300 mm) (40% of the full height); specimen 1A, with a nib height of 15 in. (380 mm) (50% of the full height); and specimen 8B, with a nib height of 24 in. (610 mm) (80% of the full height). Specimens 1A and 8A had the same dapped-end reinforcement, while specimen 8B was constructed without hanger and shear friction reinforcement. **Figure 21** shows the failure modes for specimens 1A, 8A, and 8B. Test results indicated that the failure mode was affected by the nib height. Specimen 1A, with a nib height of 15 in., failed due to concrete crushing at the bottom corner of the web. Specimen 8A, with a reduced nib height of 12 in., experienced a diagonal cracking failure in the nib

section. Clearly, reducing the nib section height increased the shear stresses within the nib section, which resulted in a nib failure.

Specimen 8B, without hanger and shear friction reinforcement, was tested to examine the hypothesis that dapped-end reinforcement is not necessary if the height of the dap (notch) is less than or equal to 20% of the full member height. This specimen failed due to a diagonal crack emanating from the reentrant corner and propagating up to the web-flange junction. The failure did not engage the full depth of the section, presumably due to the absence of the hanger reinforcement. However, specimen 8B without dap reinforcement achieved the required ultimate strength, like specimen 1A. The failure load of specimen 8B was 44.3 kip (197 kN), well over the required factored design load, confirming the adequacy of using a reinforced bearing scheme without dap reinforcement for shallow daps (notches) less than or equal to 20% of the full height of the member.

Specimen 10B with the pocket nib configuration also experienced diagonal tension failure within the nib as expected due to high shear stresses within the nib section.

Seven parameter: Splice length of hanger reinforcement

The splice between the hanger reinforcement tails and pretensioning strand was investigated in a separate experimental program, which is included in the research report.⁷ The effect of this parameter was further investigated by comparing specimen 9B, which had a splice length of 15 in. (380mm) ($0.94\ell_d$, where ℓ_d is the development length); specimen 1A, which had a splice length of 36 in. (910 mm) ($2\ell_d$); and specimen 9A, which had a splice length of 60 in. (1500 mm) ($3.75\ell_d$). The development length ℓ_d of the no. 5 (16M) hanger bars was calculated for each specimen using the measured material properties for the concrete and the steel reinforcement. Significant differences in the behavior were observed among these three specimens. Specimen 9B, with the shortest splice length, failed due to flexure-shear cracking that was precipitated by longitudinal splitting and bond failure at the bottom of the stem in the splice zone. This was expected because of the short splice length and termination of the extension of the hanger steel within a distance less than the transfer length of the strand. Specimens 1A and 9A both failed at higher loads due to concrete crushing at the bottom corner of the web. Apparently, increasing the splice length in specimen 1A to 36 in., which is greater than the strand prestress transfer length of 28 in. (710 mm) and approximately twice the bar development length, prevented the premature failures precipitated by splitting. **Figure 22** plots the load versus the vertical deflections for specimens

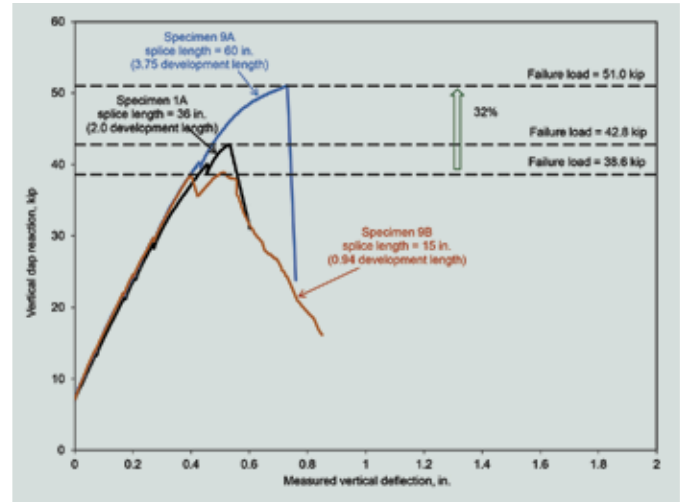


Figure 22. Measured vertical deflections for specimen 1A (36 in. splice), specimen 9A (60 in. splice), and specimen 9B (15 in. splice). Note: 1 in. = 25.4 mm; 1 kip = 4.448 kN.

1A, 9A, and 9B. Specimen 9A, which had the longest splice ($3.75\ell_d$), exhibited a 32% increase in the ultimate strength compared with 9B, which had the shortest splice ($0.94\ell_d$). The difference in ultimate capacity between specimens 1A and 9A is mainly attributable to the lower compressive strength of the concrete in specimen 1A and the shallower side cover on its hanger bars. It is doubtful that a longer tail length in specimen 1A would have substantially improved its performance.

Conclusion

The experimental program presented in this paper is part of a larger research effort. The research effort also included an extensive analysis using three-dimensional nonlinear finite element modeling and rational analysis, which resulted in the development of design guidelines for dapped ends of prestressed concrete thin-stemmed members. A companion paper¹¹ presents the design guidelines. The experimental program consisted of testing full-scale dapped-end single-tee-beam specimens to examine the performance of six selected reinforcement schemes for the dapped ends and to study the influence of six additional parameters believed to have significant effects on the behavior. Several conclusions were drawn based on the results of the experimental program. These conclusions apply to the dapped ends of prestressed concrete thin-stemmed members:

- Initiation of the first crack always occurred at the reentrant corner of most dapped ends due to high stress concentration at this location. Cracking at service load can be reduced by extending the prestressing strand through the nib, use of the inclined L scheme, and use of a corner angle.

- Four failure modes in the dapped-end region were observed:
 - formation and widening of diagonal tension cracks within the web of the full-depth section of the beam
 - formation of flexure-shear cracking in the full-depth section of the beam precipitated by longitudinal splitting of the web and strand bond failure
 - crushing of the concrete of the diagonal strut in the hanger reinforcement bend region near the bottom corner of the stem
 - formation of diagonal tension cracks within the nib, especially if the nib height is less than 50% of the full height of the member
- All six reinforcement schemes are suitable for use in practice, with ultimate capacities exceeding the factored design load by 35% to 74%.
- The inclined L scheme exhibited superior strength and serviceability compared with other schemes because the hanger reinforcement is nearly parallel to the diagonal tension field.
- The vertical C scheme cannot arrest diagonal tension cracking within the nib and could lead to failure due to the formation of a diagonal tension crack within the nib that extends upward and runs around the upper bend region of the C bar.
- The custom WWR scheme exhibited weak performance in terms of strength and crack control. Eccentric location of the WWR could result in wider cracks on one face of the web compared with the opposite face.
- Proper detailing and placement of the reinforcement for dapped ends is important to prevent splitting failures due to inadequate concrete covers.
 - Extending at least two fully tensioned prestressing strands through the nib increases the ultimate capacity of the dapped end by precompressing the mid-depth region of the web. Prestressing the nib is also effective in reducing both the extent and the width of cracks at service load.
 - Increasing the concrete strength increases the strength of the end region, but not in direct proportion to the square root of the concrete strength.
 - Increasing shear reinforcement of the web increases strength and ductility after cracking; however, it does not prevent the sudden nature of failure.
 - The splice length between the hanger reinforcement tails and pretensioning strand must be sufficient to avoid premature splitting of the thin stems.

Design guidelines consistent with these findings are provided in part 2 of this paper.¹¹

Acknowledgments

The authors would like to thank the PCI Research and Development (R&D) Committee for sponsoring this research. They are grateful for the support and guidance provided by the R&D industry advisory group, which was formed in 2011, throughout all phases of this research project. Both Tindall Corp. and Metromont Corp. made substantial contributions by donating test specimens, materials, and expertise in support of this experimental program. Special acknowledgment is extended to Don Logan and Alan Mattock for their interest, in-depth discussions, and guidance provided to the research team during this research. In addition, Logan Structural Research Foundation provided funding for a prior experimental program on dapped beams at North Carolina State University (NCSU), the results of which were especially beneficial for this research. Finally, the authors are grateful to Blake Andrews and Kurt Holloway of Wiss, Janney, Elstner Associates Inc. for their participation, as well as to the staff and students at the Constructed Facilities Laboratory at NCSU for their help throughout the experimental program.

References

1. PCI Industry Handbook Committee. 2010. *PCI Design Handbook: Precast and Prestressed Concrete*. MNL-120. 7th ed. Chicago, IL: PCI.
2. Mattock, A. H., and T. C. Chan. 1979. "Design and Behavior of Dapped-End Beams." *PCI Journal* 24 (6): 28–45.
3. Mattock, A. H., and T. S. Theryo. 1986. "Strength of Precast Prestressed Concrete Members with Dapped Ends." *PCI Journal* 31 (5): 58–75.
4. Nanni, A., and P.-C. Huang. 2002. "Validation of an Alternative Reinforcing Detail for the Dapped Ends of Prestressed Double Tees." *PCI Journal* 47 (1): 38–50.
5. Forsyth, M. B. 2013. "Behavior of Prestressed Precast Concrete Thin-Stemmed Members with Dapped Ends." MS thesis. Department of Civil, Construction and Environmental Engineering, North Carolina State University (NCSU), Raleigh, NC.
6. Botros, A. 2015. "Behavior and Design of Dapped Ends of Prestressed Concrete Thin-Stemmed Members." PhD diss., Department of Civil, Construction and Environmental Engineering, NCSU, Raleigh, NC.
7. Klein, G., B. Andrews, and K. Holloway. 2015. *Development of Rational Design Methodologies for Dapped Ends of Prestressed Concrete Thin-Stemmed Members*. WJE no. 2011.3373. Northbrook, IL: Wiss, Janney, Elstner Associates Inc.
8. Raths, D. 2008. *Double Tee Dapped End Problems: Thin Stem Members*. PCI Technical Activities Committee report. Chicago, IL: PCI
9. Abdie, J. L., and A. H. Mattock. 1988. "Transfer of Force between Reinforcing Bars and Pretensioned Strand." *PCI Journal* 33 (3): 90–106.
10. Mattock, A. H. 2012. "Strut-and-Tie Models for Dapped-End Beams." *Concrete International* 34 (2): 35–40.
11. Klein, G., A. Botros, B. Andrews, and K. Holloway. "Dapped Ends of Prestressed Concrete Thin-Stemmed Members: Part 2, Design." *PCI Journal* 62 (2): 83–100.
12. ACI (American Concrete Institute). 2014. *Building Code Requirements for Structural Concrete (ACI 318-14) and Commentary (ACI 318R-14)*. Farmington Hills, MI: ACI.

Notation

| | | |
|-----------|---|---|
| A_h | = | area of shear friction reinforcement across vertical crack at dapped ends and corbels |
| A_s | = | area of nib flexural reinforcement |
| A_{sh} | = | area of hanger reinforcement |
| A'_{sh} | = | area of horizontal extension of hanger reinforcement |
| A_v | = | area of diagonal tension reinforcement |
| D | = | dead load |
| f'_c | = | compressive strength of concrete |
| ℓ_d | = | development length in tension of deformed bar |
| L | = | live load |
| N_u | = | factored horizontal dap reaction |
| S | = | snow load |
| V_u | = | factored vertical dap reaction |

About the authors



Amir W. Botros, PhD, is an assistant professor of structural engineering at Ain Shams University in Egypt. He earned his PhD from North Carolina State University (NCSU) in Raleigh, N.C. He earned his BSc and MSc from Ain Shams University in Egypt.



Gary J. Klein is executive vice president and senior principal for Wiss, Janney, Elstner Associates Inc. in Northbrook, Ill.



Gregory W. Lucier, PhD, is a research assistant professor in the Civil, Construction and Environmental Engineering department and manager of the Constructed Facilities Laboratory at NCSU.



Sami H. Rizkalla, PhD, FPCI, FACS, FASCE, FIIFC, FEIC, FCSCE, is a Distinguished Professor of Civil Engineering and Construction, director of the Constructed Facilities Laboratory, and director of the NSF Center for Integration of Composites into Infrastructure at NCSU.



Paul Zia, PhD, is a Distinguished University Professor Emeritus at NCSU.

Abstract

This paper describes the behavior of dapped ends of prestressed concrete thin-stemmed members based on an extensive experimental program conducted to identify the most effective reinforcement schemes and develop design guidelines for dapped ends. Experimental research findings presented in this paper were used to develop design guidelines that are presented in a companion paper.

Each end of 10 full-scale single-tee prestressed concrete beams with dapped ends was tested to failure (20 tests in total). Six different reinforcement schemes were investigated in the experimental program: the vertical L, inclined L, vertical Z, custom welded-wire reinforcement, vertical C, and CZ schemes. The experimental program also examined the influence of several parameters believed to affect the behavior, including the prestressing of the nib, concrete strength, web shear reinforcement, nib height, and splice length of the hanger reinforcement. The experimental results indicated that the extent of cracking at service load, the ultimate strength, and the failure mode are influenced by the reinforcement arrangement at the dapped end. Service load cracking can be controlled to acceptable levels through proper design and detailing of the reinforcement within the end region.

Keywords

Behavior, dapped ends, prestressed concrete thin-stemmed members, reinforcement schemes, service load cracking.

Review policy

This paper was reviewed in accordance with the Precast/Prestressed Concrete Institute's peer-review process.

Reader comments

Please address reader comments to journal@pci.org or Precast/Prestressed Concrete Institute, c/o *PCI Journal*, 200 W. Adams St., Suite 2100, Chicago, IL 60606. ¶